Experimental study of resin coating to improve the impact strength of fused filament fabrication process pieces

Luis Lisandro López Taborda
Department of Mechanical Engineering, Universidad del Atlantico, Barranquilla, Colombia; Department of Mechanical Engineering, Universidad del Norte, Barranquilla, Colombia and Department of Development, Research and Innovation, 3D Ingenieria BQ SAS, Barranquilla, Colombia

Eduar Pérez and Daniel Quintero
Department of Mechanical Engineering, Universidad del Norte, Barranquilla, Colombia and Department of Mechanical Engineering, Universidad Francisco de Paula Santander-Ocaña, Ocaña, Colombia

José Fernando Noguera Polania, Habib Zambrano Rodriguez and Heriberto Maury
Department of Mechanical Engineering, Universidad del Norte, Barranquilla, Colombia, and

Ivan E. Esparragoza
Department of Engineering, Penn State Brandywine, Media, Pennsylvania, USA

Abstract

Purpose – This study aims to evaluate the impact breaking energy of the parts manufactured by the fused filament fabrication (FFF) method. The evaluation considers the use of the epoxy resin coating, different materials and different printing orientations.

Design/methodology/approach – The authors developed an experimental statistical design using 54 experimental trials. The experiments' output variable is the impact break energy of the parts manufactured by the FFF method. The input variables for the experiments consist of an epoxy resin coating (XTC-3D®, generic resin and without resin coating), different filament materials (nylon + carbon fiber, polyethylene terephthalate and polycarbonate) and different printing orientations (flat, edge and vertical) used. The authors carried out the tests following the EN ISO 179-1.

Findings – The use of resin coating has a significant influence on the impact energy of parts manufactured using the FFF method. The resin coating increases the impact resistance of parts processed by FFF by almost 100% of the value as compared to the parts without a resin coating. Post-processing is useful on ductile materials and increases impact breaking energy at weak print orientations.

Originality/value – This research opens a new opportunity to improve the mechanical properties of parts manufactured using the FFF method. The use of a resin coating reinforces the parts in weak print orientation.

Keywords Fused deposition modeling, Fused filament fabrication, Impact break energy, Impact strength, Resin coating

Paper type Research paper

1. Introduction

Additive manufacturing (AM) is a manufacturing technology with many advantages over conventional processes. For example, some of the advantages include the manufacture of complex shapes without cost increases, the minimum requirement of tools or workers and the direct relationship between design and manufacturing, among others. Because of these advantages, the use of AM is increasing rapidly, and more researchers are interested in studying how to improve the AM process to achieve quality products. One of the biggest challenges is that products manufactured by AM are anisotropic, with slightly lower mechanical properties than products manufactured by conventional processes. Consequently, this work presents the results of an experiment to improve the impact energy of parts created by AM using a resin coating. The experiment includes two additional variable factors: the orientation of the impression and the specific material. This work is significant because of the need to produce mechanical parts by using the fused filament

The current issue and full text archive of this journal is available on Emerald Insight at: **https://www.emerald.com/insight/1355-2546.htm**

Rapid Prototyping Journal
27/3 (2021) 475–486

[DOI 10.1108/RPJ-08-2018-0194]

This work was supported by the Universidad del Norte and the call for proposal of Colciencias No. 727 and 753, and also by the Universidad del Atlántico by call for proposal RES001735. The experimental data were obtained at the Universidad del Norte and 3D Ingeniería Bq SAS.

Received 7 August 2018
Revised 22 February 2019
30 May 2019
4 October 2019
13 January 2020
11 June 2020
Accepted 23 September 2020

fabrication (FFF) method. This article contains six sections: state of the art, experimental design, experimental results and statistical analysis, fracture analysis, discussion of results and conclusions and future work.

2. State of the art

The literature identifies different ways to increase the mechanical strength and impact strength of parts manufactured by FFF. Some of the methods focus on the pre-processing period (pre-processing), other methods focus on the period during the process and other methods focus on the post-processing period (post-processing).

For the methods focusing on the pre-processing period (pre-processing), many researchers added a specific component to the filament to improve the original one. Weng *et al.* (2016) reinforced acrylonitrile butadiene styrene (ABS) filaments with organic nano-compounds. They manufactured the filament in a single screw extruder and used to make parts by FFF for tensile and flexural tests, thermal expansion and dynamic tests. The results showed that the addition of 5% of the nano compound improved the tensile strength of the samples by 43% as compared to the samples made with the original ABS filament. There was a significant increase in tensile modulus, flexural strength, flexural modulus and dynamic storage modulus. However, the implementation of these methods requires additional machines to manufacture the filament and add additives.

Regarding the methods that focus on the process, Wang *et al.* (2017) studied the influence of the height of the layer (0.2 and 0.4 mm) and the temperature of the bed of impression (30 and 160°C) on the Izod impact strength of polylactic acid (PLA) manufactured by fused deposition modeling (FDM). X-ray diffraction analysis and polarized light microscope observations confirmed the influence of bed temperature on the crystal structure of PLA, and at higher temperatures, the impact strength increases. The impact fracture energy was higher compared to the samples made by plastic injection, and even higher than the samples made by FDM at low temperature. Sood *et al.* (2010) made a mechanical characterization (tensile, flexural and Charpy impact tests) of the ABS samples manufactured by FDM considering the height of the layer, the orientation, the raster angle, raster width and air gap (fill density). They obtained the regression models of the different outputs and found the exact parameters to improve the printed parts. Tsouknidas *et al.* (2016) manufactured PLA samples by FDM. They varied the height of the layer (0.1, 0.2 and 0.3 mm), the filling density (25, 50 and 100%) and the filling pattern (rectilinear, orthogonal and concentric). They performed an impact test (Instron 9350 Drop Tower) on samples with a cylindrical shape. The filling density was very significant in the force and impact energy. The height of the layer was significant in the output variables. The samples absorbed the highest impact energy for the cases with the lowest filling density and the lowest height of the layer. Dawoud *et al.* (2016) investigated the tensile strength, impact strength and flexural strength of ABS parts manufactured by FFF and plastic injection, for parts manufactured by FFF changing the raster angle and the air gap (fill density). They concluded that with proper parameters, they could obtain mechanical properties comparable to those of plastic injection molded samples. The best results for traction and impact were for a −45°/+ 45° raster orientation, while for flexion, the best results were for 0°/90°. Caminero *et al.* (2018) used a double extruder in the FFF process, to combine nylon (PA) with fiberglass and carbon fiber (CF) (Kevlar®) and studied the effect of the reinforcement of fiber in the impact strength (Charpy). The researchers experimented with different fiber contents, the height of layer and print orientation, and used a scanning electron microscope to analyze failure mode and fracture. The results of impact tests on samples without reinforcement showed that increasing the height of the layer increases the impact strength in flat samples, but the behavior is reversed in the samples at the edge. While this trend is reversed in cases with reinforced samples, in general, the impact strength increases with the fiber content.

For the post-process focusing methods, Benwood *et al.* (2018) investigated the influence of extrusion temperature, print bed temperature, raster angle and annealing, in the impact, tensile and flexural strengths of PLA samples made by plastic injection and FDM. They concluded that at high temperatures of the printing bed, the crystallinity increased, and this also increased the resistance of the material (at 105° C compared to the printed samples at 60°C). They obtained the best results of resistance to impact after the annealing (annealing treatment at 100 and 80°C for 1 h). Jo *et al.* (2016) proposed resin infiltration in parts manufactured by FDM, to improve surface finish, tightness, shrinkage and mechanical strength (tensile test). They compared the results obtained by this method with other methods such as immersion and fumigation with acetone before and after the subsequent treatment. They found that the proposed method provides the maximum force, higher than that of untreated samples, and that of samples treated by other methods. Hsu *et al.* (2010) developed a prosthetic socket for a patient with transtibial amputation. They manufactured a polycarbonate (PC) socket by FFF. After covering the preliminary socket with several layers of cotton socks, the procedure mixes unsaturated polyester resin (UPR) with a hardener and then uniformly fills and squeezes the liquid by hand around the socket to allow the UPR to infiltrate the fiber layers of the socks. This step uses a vacuum pump to maintain the lamination and curing process for 3 h continuously. The socket was covered with cotton socks and impregnated with UPR to prevent breaks between the layers and increase flexural strength. To test the socket, they used a patient in a walking test to measure the pressure distribution between the socket and the stump. The pressure in the support phase was higher for reinforced socket than for others made by conventional processes. The experimental results showed that the application is possible. Roberson *et al.* (2015) investigated the influence of the FDM, FFF and machining manufacturing process on the impact strength of notched parts (ABS, PC, ABS-PC and ULTEM 9085). Other experimental factors considered the orientation of the printing and the type of equipment and materials (industrial and desktop). Impact strength was higher in flat samples, at the edge and finally in vertical samples. There were no

statistical differences in the use of industrial or desktop machinery. There was no statistical difference in the parts manufactured by FDM and the machining, but the dispersion of the data was less in FDM. In the case of PC material, the results were more dispersed because of its brittleness. The researchers suggested a new impact test standard on samples made by AM because of differences in data dispersion compared to other notch-making methods. Kannan and Senthilkumaran (2014) investigated the influence of electrodeposition treatment on ABS manufactured by FDM. They measured the hardness and impact strength of the samples. In this case, the experimental factors were the thickness of the nickel layer and the impact mass. They demonstrated that hardness and impact strength increase as nickel thickness increases.

Regardless of the reasons for the mechanical anisotropy of materials manufactured by FDM or FFF, the literature search includes different methods to improve mechanical strength after the FFF/FDM (Jo *et al.*, 2016; Benwood *et al.*, 2018; Hsu *et al.*, 2010; Kannan and Senthilkumaran, 2014), but below we include research that explains the causes of anisotropy in materials manufactured by FDM. Ahn *et al.* (2002) manufactured ABS samples by FDM and plastic injection, and tested the samples under tension and compression. In the tensile samples, the experimental factors were the air gap (0.0 mm and 0.0508 mm), the raster width, the temperature of the extruder, the color of the material and the orientation of the raster (0°, 45°/−45°, 0°/90° and 90°), and there was a statistical significance of the air gap and the orientation of the raster in the tensile strength. For the compression samples, the experimental factor was the orientation of the impression (horizontal and vertical), which significantly impacted the compression force. In general, the mechanical properties of printed parts were weaker than those of plastic injection molded parts. From these statistical results, Ahn *et al.* (2002) extracted various design rules. According to Ahn *et al.* (2002), FDM's manufacturing process produces material fibers in different directions concerning external force. These fiber orientations depend on air gap, print orientation and raster angle. The fibers of material that align with the external load, better support the load and explain the higher mechanical resistance of the specimens. Similarly, the manufacturing process produces internal stress concentrators that reduce the mechanical strength of the specimens. It also produces internal material concentrations that increase the strength of the specimens. Both stress concentrators and material concentrations depend on the air gap, print orientation and raster angle. In general, the material fibers, internal stress concentrators and internal material concentrations, concerning the orientation of the external load, explain the higher resistance of the specimens in specific printing directions while also explaining the weakness in other directions. Therefore, all this explains the anisotropy of the material.

The work presented in this article differs from others in the type of resin coating used and how we used it. For example, Jo *et al.* (2016) used epoxy resin (liquid YD-115J and epoxy curing agent tetraethylenepentamine with weight ratio of 100:13) mixed with a diluent (methyl ethyl ketone). They used a vacuum system to infiltrate the resin in pieces manufactured by FDM. On the other hand, the experiment presented here used two different epoxy resins (generic and XTC-3D®) and did not use either diluent or a vacuum system. Hsu *et al.* (2010) used UPR with a hardener and cotton socks on the surface of a PC socket that was manufactured by FFF, and they used a vacuum pump. The experiments presented here used a manual process without a vacuum pump. This work focuses on the impact strength and considers different printing orientations, materials and types of coating for epoxy resin.

3. Experimental design

We conducted experimental tests to investigate the effect of print orientation and an epoxy resin coating on the impact break energy of materials manufactured by FFF. This section describes the experimental variables and statistical design.

3.1 Experimental variable

The experimental factors used in this investigation are shown in Table 1. Table 2 shows the response variable and Figure 1 shows the impact test machine.

The materials printed in the experiment are used in mechanical applications because of their high mechanical resistance. We wanted to know if there was a dependency on the results based on the degree of ductility of the material. We printed the materials in different orientations because we wanted to know if the epoxy resin coating would improve the resistance in all printing directions. We used different resin types, with different hardnesses and viscosities, because we wanted to know if there was a dependency on the results based on the type of resin.

We did a non-standardized test to select the resins for the final experiment. We manufactured an ABS beam with dimensions of 80 mm long, 30 mm wide and 4 mm thick. We fixed one end of the beam and hit the other end with an 865 gr hammer that we dropped from a height of 500 mm above the

Table 1 Experimental factors

Factor	Description	Level (coding)
Material	Most of the plastics manufactured by FFF are thermoplastics. We choose thermoplastics of the rigid type in 1.75 mm diameter, filaments in 1 kg or 0.5 kg rolls	PETG, PA + CF, PC
Printing orientation	Part manufacturing orientation refers to the inclination of a part in a printing bed with respect to *X*-, *Y*- and *Z*-axis. *X*- and *Y*-axis are considered parallel to printing bed	On-edge (1), flat (2), vertical (3)*
Type of resin coating	The resin was of epoxy type and it was applied by immersion in the samples for a few seconds	Without resin coating (I), generic epoxy resin coating (II), special epoxy resin coating (III)

Note: *See Figures 3 and 4, for the printing orientation

Table 2 Response variable

Variable	Test	Standard	Variable units
The impact break energy	Charpy impact test	EN ISO 179-1	J

Figure 1 Impact test machine type Charpy

end. We chose the resins that allowed the beam to withstand the most blows without breaking.

We used the printing orientation in Figure 3 based on the literature consultation of different standardized tests to parts manufactured by FDM/FFF (Uddin *et al.*, 2017; Lee and Huang, 2013; McLouth *et al.*, 2017; Caminero *et al.*, 2018; Obst *et al.*, 2018; Domingo-Espin *et al.*, 2015). We chose materials manufactured by the same supplier to guarantee uniformity in the samples. We chose the specific supplier esun® because it reported the mechanical properties of its materials.

The machine used for testing corresponds to the following specifications: brand: TINIUS OLSEN; measurement range: 0–407.95 J; accuracy: 0.001 J; maximum temperature 45°C; and relative humidity: 55%. The three-dimensional printing machine was the Prusa Joseph I3 MK2S, and the printing parameters are shown in Table 3. Figure 2 shows the design of the samples according to EN ISO 179–1.

3.2 Samples setups

This section describes the printing orientations and epoxy resin coating

Figure 2 Sample design according to EN ISO 179-1

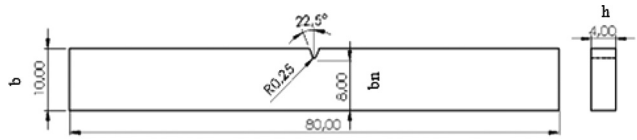

Notes: *b*, *h* and *bn* are, respectively, the width, thickness and width at the notch of the sample

3.2.1 Printing orientation

The samples have the printing orientations as shown in Figure 3.

The printing orientation generates layers oriented differently concerning the impact force, as shown in Figure 4.

3.2.2 Epoxy resin coating

There are resins in the market that improve the appearance and mechanical strength of printed parts. To verify this, we compared the impact breaking energies of samples without resin coating (I), samples with generic epoxy resin coating (II) and samples with XTC-3D® resin (III). We prepared resin II with the 1:1 volume ratios of the resin and the catalyst, respectively. We prepared resin III with 2:1 volume ratio of resin and catalyst, respectively. We prepared both

Figure 3 Printing orientation

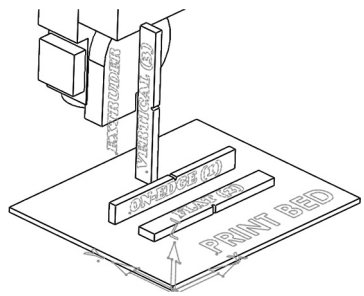

Figure 4 Printing layer orientation

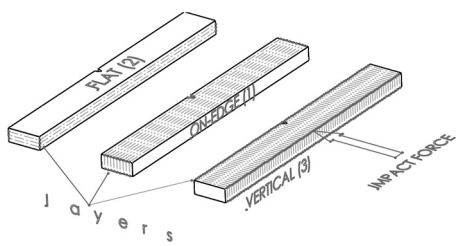

Table 3 Printing parameters

Material	Extruder temperature (°C)	Bed temperature (°C)	Nozzle diameter (mm)	Layer height (mm)	Print speed (mm/s)	Filling density (%)	Perimetral layers
PETG	240	90	0.4	0.2	40	100*	3
PA + CF	260	100	0.4	0.2	40	100*	3
PC	260	100	0.4	0.2	40	100*	3

Note: *The fill was rectilinear to +45°/−45° for all the printed samples

resins according to the manufacturer's instructions. After preparing the resins, we applied the resin by immersing the samples for a few seconds into the resin. Curing time was 24 h at a temperature of 25°C. In Table 4, we find the resins' specifications.

3.3 Statistical design

The statistical design was according to Montgomery's theory (Montgomery, 2004), and we used statistical software for design and calculations. There were three experimental blocks, one for each polyethylene terephthalate glycol (PETG), PC and PA + CF material. For each material, we changed the orientation of the printing on-edge (1), flat (2) and vertical (3), according to Figure 3. Additionally, we added different types of resin coating to printed parts, generic epoxy resin coating (II) and special epoxy resin coating (III) but included experiments without resin coating (I). We included a replica of all experiments to give statistical reliability to the experiment. We measure the impact break energy, and the size of the samples, and calculate the impact strength (see Table 5) and thickness of the resin coating (see Table 6).

The statistical analysis realized by an experimental block (for each material) included two categorical factors (the orientation of the impression and the resin coating) with three levels each. We select this type of design and analysis because the standard deviation of the energy of impact rupture is different for each material. Roberson *et al.* (2015) reported something similar. We included a co-variable analysis of the resin's height in all directions because of the variability of the resin's thickness.

Table 4 Specification of the resins

Properties/specification	Resin II	Resin III
Mix ratio by volume	1A:1B	2A:1B
Density (gr/cm^3)	1.06	1.09
Pot life (min)	45	10
Cure time (h)	3	3.5
Viscosity (CPS @ 25°c)	900–1,200	350
Shore D hardness	70 D	80 D

4. Experimental results and statistical analysis

This section presents the results and the statistical analysis of the experiments.

4.1 PETG results

Tables 5 and 6 summarize the statistical design, the impact break energy, the impact strength of notched specimens and the dimension of the samples. Table 6 summarizes the resin coating's height in all directions. Table 7 shows the analysis of variance (ANOVA) of the results for the PETG.

Table 7 shows the influence of the resin coating and print orientation on the impact break energy and the impact strength. Outputs' co-variability with resin's thickness and the

Table 5 Impact break energy and the impact strength of notched specimens

		PETG					PC					PA + CF				
Printing orientation (Type)	Resin coating (Type)	Impact break energy (J)	Impact strength of notched specimens* (kJ/m^2)	*b* mm	*h* mm	*bn* mm	Impact break energy (J)	Impact strength of notched specimens* (kJ/m^2)	*b* mm	*h* mm	*bn* mm	Impact break energy (J)	Impact strength of notched specimens* (kJ/m^2)	*b* mm	*h* mm	*bn* mm
1, on-edge	I, without	0.1371	4.1273	9.77	4.02	8.27	0.137	4.02913	10.03	4.17	8.16	1.1687	26.0697	10.18	5.00	8.96
1	I	0.1371	4.0721	9.84	4.05	8.32	0.137	4.001479	9.99	4.10	8.36	1.1687	28.0152	10.10	5.01	8.33
2, flat	I	0.4116	13.1214	10.01	3.69	8.49	0.412	11.78754	10.11	4.02	8.69	0.8242	21.3210	10.88	4.24	9.11
2	I	0.4116	12.4999	10.39	3.83	8.59	0.48	14.12765	10.08	4.02	8.45	0.8931	22.3364	10.76	4.20	9.52
3, vertical	I	0.1371	4.2041	10.05	3.87	8.43	0.137	3.739413	10.19	4.46	8.23	0.2057	4.6828	10.62	4.65	9.45
3	I	0.1371	4.1817	10.06	3.92	8.36	0.137	3.691129	10.15	4.53	8.19	0.3430	8.1070	10.70	4.49	9.43
1	II, generic	0.2743	5.9261	11.19	4.68	9.88	0.206	5.326754	10.22	4.42	8.74	0.8931	15.8174	11.25	5.31	10.63
1	II	0.4803	10.1831	11.55	4.54	10.40	0.206	4.712918	10.11	4.63	9.42	0.9620	17.5922	10.90	5.28	10.36
2	II	0.2057	4.5849	11.27	4.32	10.39	0.549	13.12292	10.13	4.76	8.80	1.5139	26.0942	12.60	5.00	11.60
2	II	0.4803	10.1703	11.88	4.19	11.28	0.618	15.06196	10.15	4.39	9.34	1.0308	15.3044	13.52	5.26	12.80
3	II	0.2743	5.7295	11.41	4.56	10.51	0.343	7.185579	10.54	4.95	9.64	0.2057	4.2691	10.67	4.92	9.80
3	II	0.4116	8.3073	11.61	4.59	10.79	0.274	5.966037	10.56	4.90	9.38	0.1371	2.5122	11.87	4.83	11.31
1	III, special	0.1371	3.5062	10.12	4.41	8.87	0.137	3.08461	10.07	4.94	9.00	0.7554	13.1916	10.17	5.89	9.72
1	III	0.2057	4.1501	11.56	4.74	10.46	0.274	6.314384	10.66	4.72	9.21	1.0998	16.8452	11.34	5.97	10.93
2	III	0.1371	2.8182	10.25	5.08	9.57	0.618	13.95015	10.58	4.38	10.10	1.0308	16.6473	12.85	5.14	12.05
2	III	0.2057	4.1947	12.06	4.40	11.14	0.48	12.06444	10.12	4.64	8.58	1.0998	23.2858	10.97	4.69	10.06
3	III	0.1371	2.7836	10.21	5.34	9.22	0.206	4.929386	10.43	4.76	8.77	0.2057	3.8248	11.54	4.78	11.24
3	III	0.1371	2.8579	10.57	5.05	9.49	0.137	3.165703	10.23	4.85	8.92	0.2057	3.5655	11.79	5.14	11.22

Note: *We convert to the units kJ/m^2 for the specific sample area $bn \times h$ according to EN ISO 179-1

Table 6 Height resin coating in mm

Resin (type)	Position (type)	PETG Mean	PETG SD**	PA + CF Mean	PA + CF SD	PC Mean	PC SD**	Height resin coating	PETG Mean	PETG SD**	PA + CF Mean	PA + CF SD**	PC Mean	PC SD**
II, generic	1, On edge	0.66	0.33	0.51	0.39	0.23	0.17	*tb**	0.51	0.42	0.63	0.43	0.10	0.09
	2, Flat	0.18	0.14	1.01	0.50	0.18	0.14	*th**	0.30	0.03	0.25	0.18	0.23	0.04
	3, Vertical	0.73	0.39	0.34	0.20	0.35	0.26	*tbn**	0.77	0.46	0.97	0.44	0.44	0.20
III, special	1, On edge	0.68	0.49	0.54	0.27	0.32	0.13	*tb**	0.27	0.21	0.45	0.13	0.13	0.05
	2, Flat	0.38	0.25	0.59	0.26	0.25	0.13	*th**	0.39	0.23	0.34	0.13	0.25	0.10
	3, Vertical	0.48	0.43	0.53	0.35	0.18	0.12	*tbn**	0.52	0.15	0.87	0.03	0.38	0.05

Notes: *tb, th and tbn are the height resin coating along the b width, the thickness h and the width of the la notch bn, respectively, and are determined based on the difference of dimensions of samples with resin and without resin from Table 5. ** SD is standard deviation

Table 7 PETG ANOVA*

Source	Impact break energy Sum of squares	DF**	Mean squares	*F*-value	*p*-value	Impact strength of notched specimens Sum of squares	DF**	Mean squares	*F*-value	*p*-value
Co-variables										
tb	0.0403	1	0.0403	75.03	0.0001	17.7633	1	17.7633	78.97	0.0001
th	0.0157	1	0.0157	29.22	0.0017	8.7091	1	8.7091	38.72	0.0008
tbn	0.0499	1	0.0499	92.98	0.0001	21.1144	1	21.1144	93.87	0.0001
Principal effects										
A: Printing orientation	0.0242	2	0.0121	22.5	0.0016	9.9926	2	4.9963	22.21	0.0017
B: Resin coating	0.0190	2	0.0095	17.68	0.0031	10.9717	2	5.4858	24.39	0.0013
Interactions										
AB	0.1140	4	0.0285	53.1	0.0001	77.3690	4	19.3423	85.99	0.0000
Residuals	0.0032	6	0.0005			1.3496	6	0.2249		
Total (corrected)	0.2934	17				192.2360	17			

Notes: *Calculated with the StatGraphics. **DF is degree of freedom

importance of the interaction between the resin and the orientation is observed. Figure 5 shows that the samples at the edge (1) and the vertical ones (3) impregnated with the generic resin (II) have higher break energy and strength than the without resin samples (I).

4.2 Nylon + carbon fiber results

Table 5 shows the results obtained in the experiment and Table 8 shows the ANOVA of the results for PA + CF.

Table 8 shows that the resin coating and print orientations significantly influence the impact break energy and the impact strength. The co-variability of the outlets with the thickness of the resin is also observed. Table 8 shows that the flat samples (2) impregnated with the generic (II) and special resin (III) have higher break energy than the flat samples (2) without resin (I). In Figure 6(b), the impact strength is higher in the samples with orientation on edge (1) and without resin (I).

4.3 Polycarbonate results

Tables 5 and 6 show the results obtained in the experiment, and Table 9 shows the ANOVA of the results for PC.

Table 9 shows that the resin coating and the orientation of the impression influence significantly the impact break energy, while the orientation of the impression influences the impact strength. There is no co-variability of the outlets with the thickness of the resin in either direction. Figure 7(a) shows that the impact break energy and impact strength of the samples with generic (II) and special (III) resins have similar values in the edge orientation (1) and the flat orientation (2), and they are larger than the sample without resin (I). In Figure 7(b), the impact strength for the generic resin (II) and without resin (II) are similar in the edge orientation (1) and the flat orientation (2) and are higher than the samples without resin (I) in the flat orientation (2).

5. Analysis of the fracture

The fractured samples were photographed to visualize the orientation of the fracture. Figures 8(a) and 10(a) show in vertical samples that the crack is parallel to the impression layer, regardless of the material. Figure 8(a) shows the PETG's fracture in the impact zone. It follows a cross pattern through several impression layers. On the other hand, Figure 9(a) shows for the PA + CF in the impact zone that the crack follows a pattern almost parallel to the impression layer and is the same for the resin-coated sample in Figure 9(b). Figure 8(a) shows that the number of fractured layers for the vertical resin coated samples is less than that of the non-resin-coated samples in the same figure.

Figure 9(b) shows that for flat PA + CF samples, the crack follows an almost straight pattern, regardless of whether it has resin. It is similar to the vertical samples in Figure 9(a). On the

Figure 5 Interaction graph for PETG

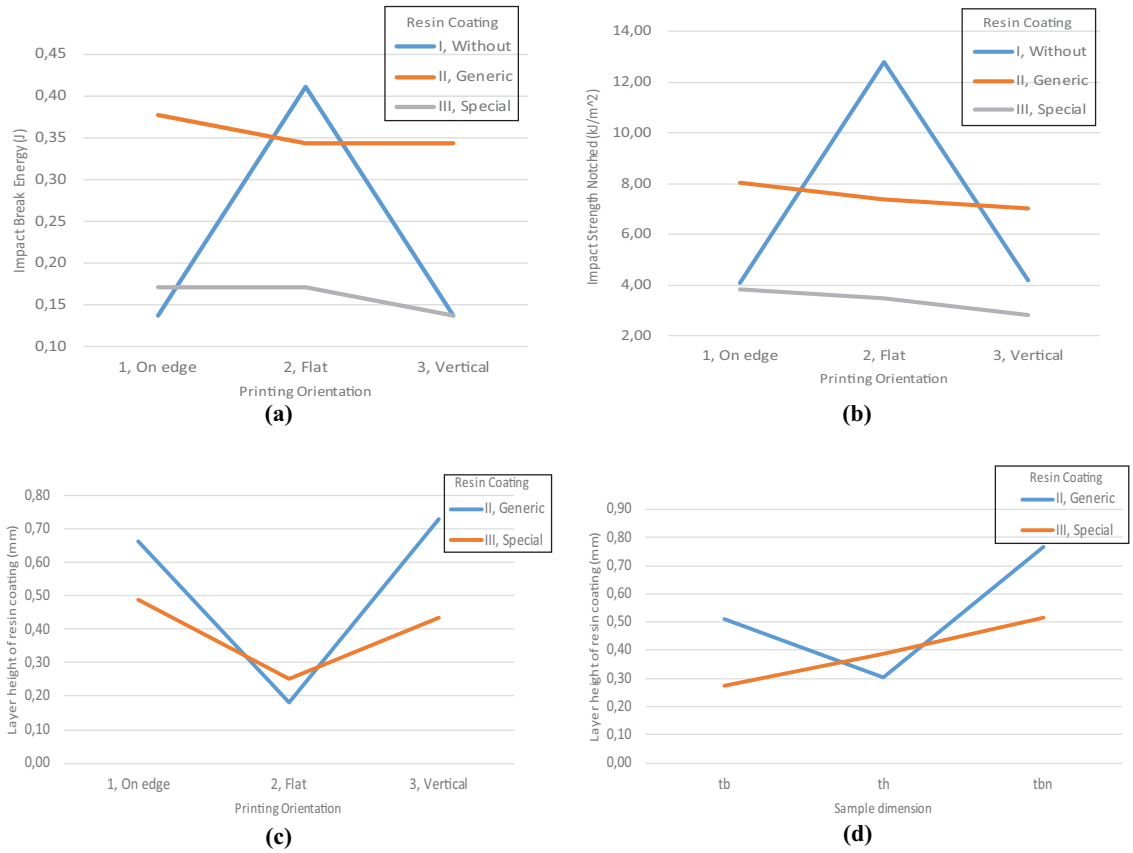

Notes: (a) Impact Break Energy vs Printing Orientation; (b) impact strength vs printing orientation; (c) height resin coating vs printing orientation; (d) height resin coating vs sample dimension

Table 8 PA + CF ANOVA

	Impact break energy					Impact strength of notched specimens				
Source	**Sum of squares**	**DF**	**Mean squares**	**F-value**	***p*-value**	**Sum of squares**	**DF**	**Mean squares**	**F-value**	***p*-value**
Co-variables										
tb	0.1165	1	0.1165	11.86	0.0137	33.5905	1	33.5905	9.61	0.0211
th	0.0886	1	0.0886	9.02	0.0239	38.1964	1	38.1964	10.93	0.0163
tbn	0.1160	1	0.1160	11.81	0.0138	37.5111	1	37.5111	10.73	0.0169
Principal effects										
A: Printing orientation	1.2898	2	0.6449	65.68	0.0001	542.575	2	271.288	77.6	0.0001
B: Resin coating	0.1371	2	0.0686	6.98	0.0271	37.9951	2	18.9975	5.43	0.045
Interactions										
AB	0.2017	4	0.0504	5.14	0.0384	56.0989	4	14.0247	4.01	0.0642
Residuals	0.0589	6	0.0098			20.9771	6	3.49618		
Total (corrected)	3.1511	17				1274.99	17			

other hand, Figure 8(b) shows in the flat samples of PETG without resin (I) that the crack begins with a slight inclination, and then as it moves away from the notch, it follows an orientation of +45° and −45° following the filling. Figures 8(b) and 9(b) show that while the resin coating is applied to the flat samples, the crack propagates straighter than without the resin coating.

6. Discussion of results

The discussion is divided into themes.

6.1 Samples without resin coating

Table 10 shows the impact strength results grouped by the orientation of the impression, material and specific research.

Figure 6 Interaction graph for PA + CF

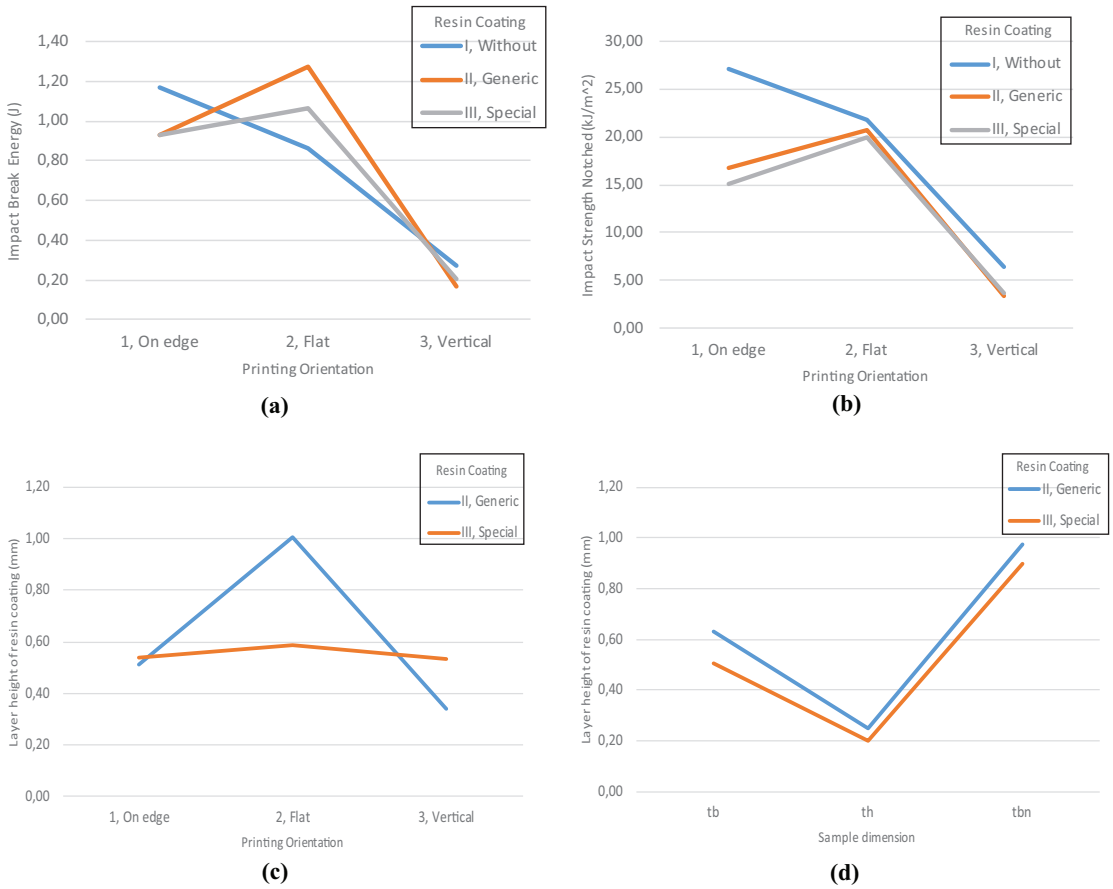

Notes: (a) Impact Break Energy vs Printing Orientation; (b) impact strength vs printing orientation; (c) height resin coating vs printing orientation; (d) height resin coating vs sample dimension

Table 9 PC ANOVA

	Impact break energy					Impact strength of notched specimens				
Source	**Sum of squares**	**DF**	**Mean squares**	***F*-value**	***p*-value**	**Sum of squares**	**DF**	**Mean squares**	***F*-value**	***p*-value**
Co-variables										
tb	0.00474	1	0.0047	5.45	0.0583	1.86111	1	1.86111	2.44	0.1697
th	0.00027	1	0.0003	0.31	0.5964	0.758666	1	0.758666	0.99	0.3576
tbn	0.00162	1	0.0016	1.86	0.2211	0.00156102	1	0.001561	0	0.9654
Principal effects										
A: Printing orientation	0.46034	2	0.2302	264.44	0.0000	301.181	2	150.591	197.04	0.0000
B: Resin coating	0.01185	2	0.0059	6.81	0.0286	6.69038	2	3.34519	4.38	0.0673
Interactions										
AB	0.00598	4	0.0015	1.72	0.2637	1.2642	4	0.316051	0.41	0.794
Residuals	0.00522	6	0.0009			4.58552	6	0.764254		
Total (corrected)	0.53015	17				327.633	17			

Table 10 shows that the impact strength is higher for flat samples (2) than for vertical samples (3). Roberson *et al.* (2015) reported that impact strength for flat samples (2) is between 100 and 494% of the value of vertical samples (3). In the experiment reported here, the impact strength of the flat samples (2) is between 300 and 313% as compared to the vertical samples (3). On the other hand, Caminero *et al.* (2018) reported that the impact strength of flat samples (2) of PA could be between 100 and 400% of the value of the edge samples (1). Roberson *et al.* (2015) reported something similar to Caminero *et al.* The impact resistance of flat samples (2) can be between 100 and 310% of the value of edge samples (1).

Figure 7 Interaction graph for PC

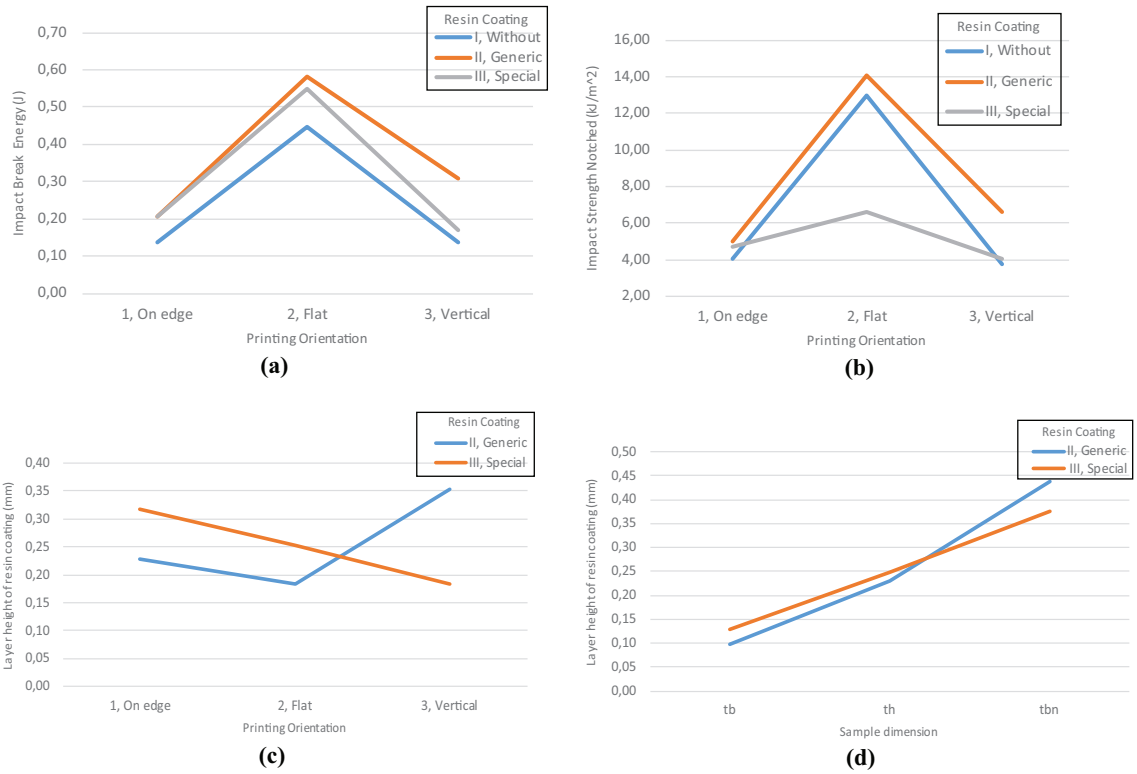

Notes: (a) Impact Break Energy vs Printing Orientation; (b) impact trength y vs printing orientation; (c) height resin coating vs printing orientation; (d) height resin coating vs sample dimension

Figure 8 Fracture of PETG samples

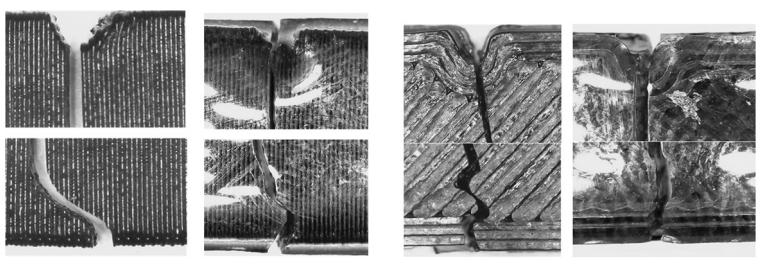

Notes: (a) Vertical (3) without (I) and Generic (II); (b) flat (2) without (I) and Generic(II)

Caminero *et al.* (2018) reported that PA edge samples reinforced with fiber (1) have higher impact strength than the flat samples (2). However, these samples have different layer height and different percentages of fiber than those used in the experiment reported in this work. In summary, the experimental results obtained for the samples without resin are similar to the results reported by other researchers.

6.2 Methods to improve impact strength

Table 11 shows each method to improve impact strength. Some methods are more effective than others: adding fiberglass reinforcement during the process improve the impact strength by 1,400%, annealing by 428%, coating with Ni by 358%, coating with epoxy resin by 196%, reducing the layer height and filling rate by 225%, overheating the print bed by 193%, optimizing the print parameters by 140% and infiltrating epoxy resin by 115%. Each method focused on different materials, mainly PLA and ABS, and in this work, PETG, PC and PA + CF. Each method considered different process parameters, such as the orientation of the impression and the height of the layer. There are other differences. For example, the resin infiltration method requires vacuum systems, the fiber reinforcement requires a dual extruder printer and the

Figure 9 Fracture of PA + CF samples

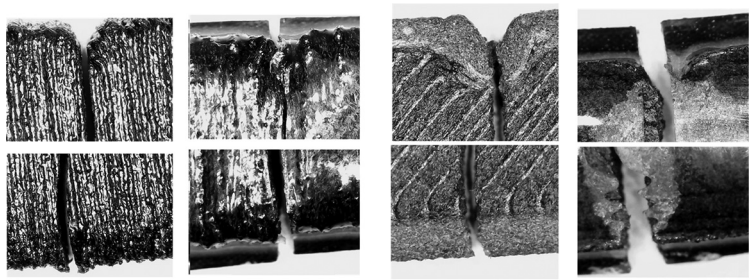

(a) **(b)**

Notes: (a) Vertical (3) without (I) and Generic (II); (b) flat (2) without (I) and Generic(II)

Table 10 Impact strength of samples without resin coating in kJ/m^2

Print orientation (type)	Present experiment			Roberson *et al.* (2015)				Caminero *et al.* (2018)			
	PETG	PA + CF	PC	ABS	PC	ABS-PC	ULTEM 9085	PA	PA + CF	PA + Kevlar Fib	PA + CF
1, On edge	4.10	27.04	4.02	3.95–8.28	2.25	9.58	3.90	10–20	24.73–82.26	36.42–184.76	86.30–280.95
2, Flat	12.81	21.83	12.96	6.52–12.26	2.31–2.89	15.15–16.52	4.028–4.975	20–40	22.21–57.50	30.11–125.47	74.16–271.19
3, Vertical	4.19	6.39	3.72	2.48–5.34	2.31	3.35	2.84				

Table 11 Improvement in impact strength for different methods

Method	% original value	Material	Ref.
Process			
Optimizing parameters	140	ABS	Sood *et al.* (2010)
Reducing infill density	225	PLA	Tsouknidas *et al.* (2016)
Fiber reinforcement	1,400	PA	Caminero *et al.* (2018)
Overheating bed	193	PLA	Benwood *et al.* (2018)
Post process			
Annealing	428	PLA	Benwood *et al.* (2018)
Coating resin	196	PETG	Present article
Coating resin	177	PC	Present article
Coating Ni	358	ABS	Kannan and Senthilkumaran (2014)
Infiltration resin	115	ABS	Jo *et al.* (2016)

annealing requires an oven for heat treatment. All these systems add additional costs that are beyond the scope of this research to analyze. Future research is recommended on the cost of each method to analyze the relationship between strength and cost.

6.3 Comparison with the conventional manufacturing processes

Table 12 shows the impact strength of materials made by FDM/FFF and the impact strength of thermoplastics made by injection molding (IM) or plastic injection. The impact strength results of the experiment using PETG with a resin coating are higher than those manufactured by IM. For the PC, the impact strength reported by the manufacturer is less than that manufactured by the IM (Mark, 2009). The impact strength results of the experiment reported in this work are lower than those of both bibliographic sources. The impact resistance for PA + CF by IM (Alfredo, 2006) is slightly higher than the values reported by esun®. The impact strength results of the experiment reported here are higher than those reported by esun®. In summary, the use of resin coating increases the impact strength, but not in all materials. It does not always exceed the impact strength of the materials manufactured by IM. The impact strength is a function of the material and the resin discussed in the next section.

Table 12 Impact strength in other manufacturing processes in kJ/m^2

Process	PETG	PC	PA + CF	PA	Source
FDM/FFF	8	48	11.5	15	eSun (Shenzhen Esun Industrial Co. Ltd, 2019)
		2.246–2.895			Roberson *et al.* (2015)
	2.82–12.81	3.72–14.09	3.39–27.04		Present experiment
IM and others				101.5	Caminero *et al.* (2018)
	8.54	9.07–16.0	9.6–13.3		Campo (Alfredo, 2006)
	9	85		5.3–6.4	Mark (2009)

Table 13 Tensile mechanical properties of the tested materials

Material	Printing orientation	*E*, Young module (MPa)	*Sy*, Yield strength (MPa)	*Su*, Tensile strength (MPa)	ϵu, Tensile deformation (%)	Ref.
PETG	Flat (2)	458	16	24	8	Szykiedans *et al.* (2017)
	Vertical (3)	910	3	6		
PA + CF	Flat (2)	4,387		118	5	Shenzhen Esun Industrial Co. Ltd (2020)
PC	Flat (2)	1,330	30	41.6	5.5	Smith and Dean (2013)
	Vertical (3)	1,570	10	17.7	1.3	

6.4 Interaction between the material and the resin coating

The results show a strong correlation between the print orientation and the resin. The most exciting and positive results are for PETG. We observed that both the impact energy and the impact strength have similar behavior for different orientations [Figure 5(a) and (b)]. When the generic resin (II) is applied, the behavior trend is isotropic. Something similar occurs with resin (III), but its average strength values are lower than those of the generic resin (II) and without samples (I). In Figure 5(b), we see an increase in impact strength in the edge (1) and vertical (3) orientations in the generic resin samples (II) compared to the samples without resin (I). That coincides with higher thickness of resin in these orientations [Figure 5(c)], in contrast to the resistance in the flat orientation (2). The flat sample has the thinnest resin with the lowest strength value, consistent with the correlation of the height or thickness of the resin layer with the impact energy of the fracture (Table 7). An explanation for the loss and gain of resistance could be related to the hardness of the resin and its layer thickness. The resin (III) is the hardest and the thinnest, reducing the ductility of the material, thus reducing the capacity to absorb the impact energy. An explanation for the behavior isotropic could be related to the difference between resin layers with printing orientation. The weak orientation, on edge (1) and vertical (3) has more layer thickness than strongest orientation, flat (2). However, to corroborate the above explanation, it is necessary to control the layer thickness and do static tests beyond the scope of this study.

The resin layer is more abundant in the notch area than concerning the resin layers in the sample thickness and width [Figure 5(d)]. The shape of the notch facilitates the accumulation of resin in that specific area. Increasing the amount of resin in the notch would explain the increase in impact breaking energy because of the increase in area. However, it would not explain the increase in impact strength, because impact strength is defined as the specific energy per unit area, not depending on the increase in area, but on the mechanical properties of the material. This behavior is similar to the findings of Kannan and Senthilkumaran (2014). They reported that the energy absorbed during impact depends on the surface's hardness, height or thickness of the coating and hammer's mass. In our experiment, the hammer mass is constant, but the way we apply the resin does not allow us to obtain a uniform height or thickness of the layer. Specific investigation of the influence of the height or thickness of the layer on energy and impact strength is beyond this work (Table 13).

7. Conclusions and future work

Parts made by FDM/FFF have lower mechanical properties than parts made by conventional processes such as IM. Furthermore, these pieces are anisotropic, so the use of printed materials is limited in cases where mechanical resistance is not critical. This research showed that:

- The orientation of the print and epoxy resin coating is significant in the impact rupture energy of parts manufactured by FFF.
- The impact break energy and behavior of parts manufactured by FFF and coated with epoxy resin are a function of the manufacturing orientation, the hardness of the resin coating, the height or thickness of the resin layer and the ductility of the material.
- Post-processing is more effective in ductile materials than brittle materials.
- The resin coating increases the impact energy even at weak print orientations of FFF manufactured parts up to 96% of value without resin coating.
- The epoxy resin coating allows equalizing the resistance of FFF materials with materials manufactured by conventional processes, even surpassing it in some cases.

We recommend in the future:

- To improve the application process of the epoxy resin to control the uniformity of the resin layer and the thickness.
- To investigate the influence of thickness, hardness and viscosity of epoxy resin on the impact break energy of parts manufactured by FFF/FDM.
- To investigate the influence of the resin on the parts without a stress concentrator or notch.
- To investigate the influence of the resin coating on the material's ductility, tensile, compression, flex and buckling properties.
- To investigate the influence of the mass of the hammer on the impact of energy and impact strength of parts manufactured by FFF/FDM.
- To investigate the costs of implementing each method to improve impact strength and compare the relationship between strength and cost.

The door is open for future investigations in the line of mechanical characterization of printed parts using resin coatings to reinforce the behavior in traction, flexion, compression, buckling, fatigue and resistance to fracture, among other properties.

References

Ahn, S.-H., Montero, M., Odell, D., Roundy, S. and Wright, P.K. (2002), "Anisotropic material properties of fused deposition modeling {ABS}", *Rapid Prototyping Journal*, Vol. 8 No. 4, pp. 248-257, doi: 10.1108/13552540210441166.

Alfredo, C. (2006), *The Complete Part Design Handbook for Injection Molding of Thermoplastics*, Hanser Gardner Publications, Inc. ISBN, OH.

Benwood, C., Anstey, A., Andrzejewski, J., Misra, M. and Mohanty, A.K. (2018), "Improving the impact strength and heat resistance of 3D printed models: structure, property, and processing correlationships during fused deposition modeling (FDM) of poly (lactic acid)", *ACS Omega*, Vol. 3 No. 4, pp. 4400-4411.

Caminero, M.A., Chacon, J.M., Garcia-Moreno, I. and Rodriguez, G.P. (2018), "Impact damage resistance of 3D printed continuous fiber reinforced thermoplastic composites using fused deposition modeling", *Composites Part B: Engineering*, Vol. 148, pp. 93-103.

Dawoud, M., Taha, I. and Ebeid, S.J. (2016), "Mechanical behavior of ABS: an experimental study using FDM and injection molding techniques", *Journal of Manufacturing Processes*, Vol. 21, pp. 39-45.

Domingo-Espin, M., Puigoriol-Forcada, J.M., Garcia-Granada, A.-A., Lluma, J., Borros, S. and Reyes, G. (2015), "Mechanical property characterization and simulation of fused deposition modeling polycarbonate parts", *Materials & Design*, Vol. 83, pp. 670-677.

Montgomery, D.C. (2004), *Design and Analysis of Experiments*, John Wiley & Sons.

Hsu, L.H., Huang, G.F., Lu, C.T., Hong, D.Y. and Liu, S.H. (2010), "The development of a rapid prototyping prosthetic socket coated with a resin layer for transtibial amputees", *Prosthetics and Orthotics International*, Vol. 34 No. 1, pp. 37-45.

Jo, K.-H., Jeong, Y.-S., Lee, J.-H. and Lee, S.-H. (2016), "A study of post-processing methods for improving the tightness of a part fabricated by fused deposition modeling", *International Journal of Precision Engineering and Manufacturing*, Vol. 17 No. 11, pp. 1541-1546.

Kannan, S. and Senthilkumaran, D. (2014), "Assessment of mechanical properties of Ni-coated ABS plastics using FDM process", *IJMME-IJENS*, Vol. 14 No. 3, pp. 30-35.

Kannan, S. and Huang, A. (2013), "Fatigue analysis of FDM materials", *Rapid Prototyping Journal*, Vol. 19 No. 4, pp. 291-299.

Lee, J. and Huang, A. (2013), "Fatigue analysis of FDM materials", *Rapid Prototyping Journal*, Vol. 19 No. 4, pp. 291-299.

Mark, J.E (2009), *Polymer Data Handbook*, Oxford university press New York, NY, available at: https://books.google.com.co/books/about/Polymer_Data_Handbook.html?id=qFi5QgAACAAJ&redir_esc=y

McLouth, T.D., Severino, J.V., Adams, P.M., Patel, D.N. and Zaldivar, R.J. (2017), "The impact of print orientation and raster pattern on fracture toughness in additively manufactured ABS", *Additive Manufacturing*, Vol. 18, pp. 103-109.

Obst, P., Launhardt, M., Drummer, D., Osswald, P.V. and Osswald, T.A. (2018), "Failure criterion for PA12 SLS additive manufactured parts", *Additive Manufacturing*, Vol. 21, pp. 619-627.

Roberson, D.A., Perez, A.R.T., Shemelya, C.M., Rivera, A., MacDonald, E. and Wicker, R.B. (2015), "Comparison of stress concentrator fabrication for 3D printed polymeric izod impact test specimens", *Additive Manufacturing*, Vol. 7, pp. 1-3.

Shenzhen Esun Industrial Co. Ltd. (2019), "Product manual esun 3D filament".

Smith, W.C. and Dean, R.W. (2013), "Structural characteristics of fused deposition modeling polycarbonate material", *Polymer Testing*, Vol. 32 No. 8, pp. 1306-1312.

Sood, A.K., Ohdar, R.K. and Mahapatra, S.S. (2010), "Parametric appraisal of the a mechanical property of fused deposition modeling processed parts", *Materials & Design*, Vol. 31 No. 1, pp. 287-295.

Szykiedans, K., Credo, W. and Osiński, D. (2017), "Selected mechanical properties of PETG 3-D prints", *Procedia Engineering*, Vol. 177, pp. 455-461.

Tsouknidas, A., Pantazopoulos, M., Katsoulis, I., Fasnakis, D., Maropoulos, S. and Michailidis, N. (2016), "The impact absorption capacity of 3D-printed components fabricated by fused deposition modeling", *Materials & Design*, Vol. 102, pp. 41-44.

Uddin, M.S., Sidek, M.F.R., Faizal, M.A., Ghomashchi, R. and Pramanik, A. (2017), "Evaluating mechanical properties and failure mechanisms of fused deposition modeling acrylonitrile butadiene styrene parts", *Journal of Manufacturing Science and Engineering*, Vol. 139 No. 8, pp. 81018

Wang, L., Gramlich, W.M. and Gardner, D.J. (2017), "Improving the impact strength of poly (lactic acid) (PLA) infused layer modeling (FLM)", *Polymer*, Vol. 114, pp. 242-248.

Weng, Z., Wang, J., Senthil, T. and Wu, L. (2016), "Mechanical and thermal properties of ABS/montmorillonite nanocomposites for fused deposition modeling 3D printing", *Materials & Design*, Vol. 102, pp. 276-283.

Corresponding author

Luis Lisandro López Taborda can be contacted at: luislopeztaborda@mail.uniatlantico.edu.co; lllopez@uninorte.edu.co; llopez@3dingenieriabq.com